Journal of Food Measurement and Characterization
https://doi.org/10.1007/s11694-018-9764-x

ORIGINAL PAPER

Hyperspectral imaging as an effective tool for prediction the moisture content and textural characteristics of roasted pistachio kernels

Toktam Mohammadi-Moghaddam[1,2] · Seyed M. A. Razavi[2] · Masoud Taghizadeh[2] · Biswajeet Pradhan[3] · Ameneh Sazgarnia[4] · Ahmad Shaker-Ardekani[5]

Received: 10 December 2017 / Accepted: 21 February 2018

Abstract

The objective of this study was to develop calibration models for prediction of moisture content and textural characteristics (fracture force, hardness, apparent modulus of elasticity and compressive energy) of pistachio kernels roasted in different conditions (temperatures 90, 120 and 150 °C; times 20, 35 and 50 min and air velocities 0.5, 1.5 and 2.5 m/s) using Vis/NIR hyperspectral imaging and multivariate analysis. The effects of different pre-processing methods and spectral treatments such as normalization [multiplicative scatter correction (MSC), standard normal variate transformation (SNV)], smoothing (median filter, Savitzky–Golay and Wavelet) and differentiation (first derivative, D^1 and second derivative, D^2) on the obtained data were investigated. The prediction models were developed by partial least square regression (PLSR) and artificial neural network (ANN). The results indicated that ANN models have higher potential to predict moisture content and textural characteristics of roasted pistachio kernels comparing to PLSR models. High correlation was observed between reflectance data and fracture force ($R^2 = 0.957$ and RMSEP = 3.386) using MSC, Savitzky–Golay and D^1, compressive energy ($R^2 = 0.907$ and RMSEP = 15.757) using the combination of MSC, Wavelet and D^1, moisture content ($R^2 = 0.907$ and RMSEP = 0.179) and apparent modulus of elasticity ($R^2 = 0.921$ and RMSEP = 2.366) employing combination of SNV, Wavelet and D^1, respectively. Moreover, Vis–NIR data correlated well with hardness ($R^2 = 0.876$ and RMSEP = 5.216) using SNV, Wavelet and D^2. These results showed the capability of Vis/NIR hyperspectral imaging and the central role of multivariate analysis in developing accurate models for prediction of moisture content and textural properties of roasted pistachio kernels.

Keywords Hyperspectral imaging · Non-destructive · Reflectance · Roasting · Texture · Vis–NIR

Introduction

Pistachio nut (*Pistacia vera* L.) is one of the most delicious and nutritious nuts in the world and is being used as a salted and roasted product or as an ingredient in desserts (baklava, halva, paste, butter etc.) [1]. Iran is the main pistachio producer in the world with about 415,531 Mt in 2014, followed by USA, Turkey and China [2]. Pistachio kernel is a good source of fat (50–60%) [3] containing considerable amount of unsaturated fatty acids (linoleic, linolenic and oleic acids).

Roasting is one of the most important food processes, which provides useful attributes to the product. One of the objectives of nut roasting is to alter and significantly enhance the flavour, texture, colour and appearance of the product. Roasting gives nuts a variety of textures and colors, increasing their crispness and making them crunchier [4–6]. Roasted nuts are widely consumed as an appetizer and used as raw materials in sweets, confectionery, chocolate and biscuits. Because of

✉ Seyed M. A. Razavi
s.razavi@um.ac.ir

1 Department of Food Science and Technology, Neyshabur University of Medical Sciences, Neyshabur, Iran

2 Department of Food Science and Technology, Ferdowsi University of Mashhad (FUM), P.O. Box: 91775-1163, Mashhad, Iran

3 School of Systems, Management and Leadership, Faculty of Engineering and IT, University of Technology Sydney, Sydney, NSW, Australia

4 Department of Medical Physics, Faculty of Medicine, Mashhad University of Medical Sciences, Mashhad, Iran

5 Pistachio Research Center, Horticultural Sciences Research Institute, Agricultural Research, Education and Extension Organization (AREEO), Rafsanjan, Iran

Published online: 26 February 2018

the deep green color of pistachio kernels, it is favored in the ice cream and pastry industries [7]. Temperature and time are the main factors controlled during industrial roasting process. But initial moisture content and air velocity also affect heat transfer rate subsequently drying and physicochemical changes in proteins [4, 8]. During roasting, moisture content of moist nuts reduces [9] and texture becomes more crumbly and fragile (less hard) [10].

Texture characteristics such as firmness of fruits relate to their mechanical properties. A large number of devices and techniques have been developed to determine the firmness of fruits and vegetables; mostly based on puncture, compression or response to shear stress, creep, or impact. Mechanical force/deformation techniques applying compression or penetration are rarely appropriate for online sorting of fruits and vegetables since they are of low speed and/or destructive [11]. Mohammadi-Moghaddam et al. [12] studied the effect of time, temperature and air velocity of roasting on textural properties of pistachio kernels. Increasing the roasting temperature decreased the fracture force, hardness, apparent modulus of elasticity and compressive energy.

In recent years, spectral imaging techniques (i.e. hyperspectral and multispectral imaging) have emerged as a powerful tool for safety and quality inspection of various agricultural commodities. Spectral imaging combines conventional imaging and spectroscopy to obtain both spatial and spectral information from the target, which is extremely useful for evaluating individual food samples. This technique has drawn tremendous interest from both academic and industrial areas, and has been developed rapidly during the past decade [13–15].

There are some published studies on the potential of hyperspectral imaging to determine physicochemical properties of nuts, grains and seeds [16–22]. However, there is no study available about the ability of hyperspectral imaging to predict the moisture content and textural attributes of pistachio kernels. The objectives of this study were (i) to apply reflectance hyperspectral imaging for non-destructive determination of moisture content and textural attributes (hardness, fracture force, apparent modulus of elasticity and compressive energy) of pistachio kernels roasted in different conditions (temperatures: 90, 120 and 150 °C; times: 20, 35 and 50 min and air velocities: 0.5, 1.5 and 2.5 m/s), (ii) to investigate the effects of different combination of pre-processing methods on predicted moisture content and textural properties of pistachio kernels.

Materials and methods

Sample preparation

Dried O'hadi pistachio nuts were supplied from a local market in Mashhad, Iran in 2012 and stored at 4 °C for further processing. The average weight ratio of kernel was 62 g/100 g of split sample. The average moisture content of pistachio kernels was measured as 2.9% (w.b.). Kernels were sorted manually to get the uniform sizes for roasting. 1 kg pistachio nuts were soaked in 5 L of 20% salt solution for 20 min [23]. After soaking, the salt solution was drained using a strainer and the excess water was removed using a cloth filter. For roasting process, 3 temperature levels (90, 120 and 150 °C), 3 time intervals (20, 35 and 50 min) and 3 air velocities (0.5, 1.5 and 2.5 m/s) were applied. Thus, in this research, 27 different treatments of roasted pistachio kernels were analyzed. Roasting was performed in an electrical oven equipped with a controller to adjust the air velocities of roasting (CIFS120, Fan Azma Gostar, Tehran, Iran). The air velocities were measured by an electronic anemometer (AM4205, Lutron company, Taiwan) having an accuracy of 0.1 m/s. After roasting, the whole kernels were allowed to cool at room temperature (20 ± 2 °C).

Moisture content determination

Moisture content of pistachio kernels was measured in triplicate using oven drying method (105 ± 2 °C) until a constant weight was reached [24]. Moisture content was measured in three replications.

Instrumental texture analysis

Instrumental texture measurements were carried out at room temperature using a texture analyzer (CNS Farnell Com, U.K.) (Fig. 1). Uniaxial compression test, using a 35 mm diameter plastic cylinder, was made on the pistachio kernels, which were mounted over a platform. The operational conditions of texture analyzer were 2 mm deformation (target value), 20 g trigger point, one cycle and 30 mm/min cross head speed. The textural parameters of kernels were expressed as fracture force (highest peak followed by a sudden drop [N]), hardness (peak compression force [N] at target deformation), apparent modulus of elasticity or initial tangent modulus (sample rigidity that is the slope of linear part of the force–deformation curve [N/mm]) and compressive energy (area under the curve for the compression that is the work [N.mm] required to attain deformation, indicative of internal strength of bonds within product) [12, 24]. Texture measurements were performed in at least four replications.

Vis/NIR hyperspectral imaging measurements

A hyperspectral imaging system (Spectrograph model: ImSpector V10, Spectral Imaging Ltd., Oulu, Finland) in the Vis–NIR range (400–1000 nm) was employed in this study. The main components of this system are: objective

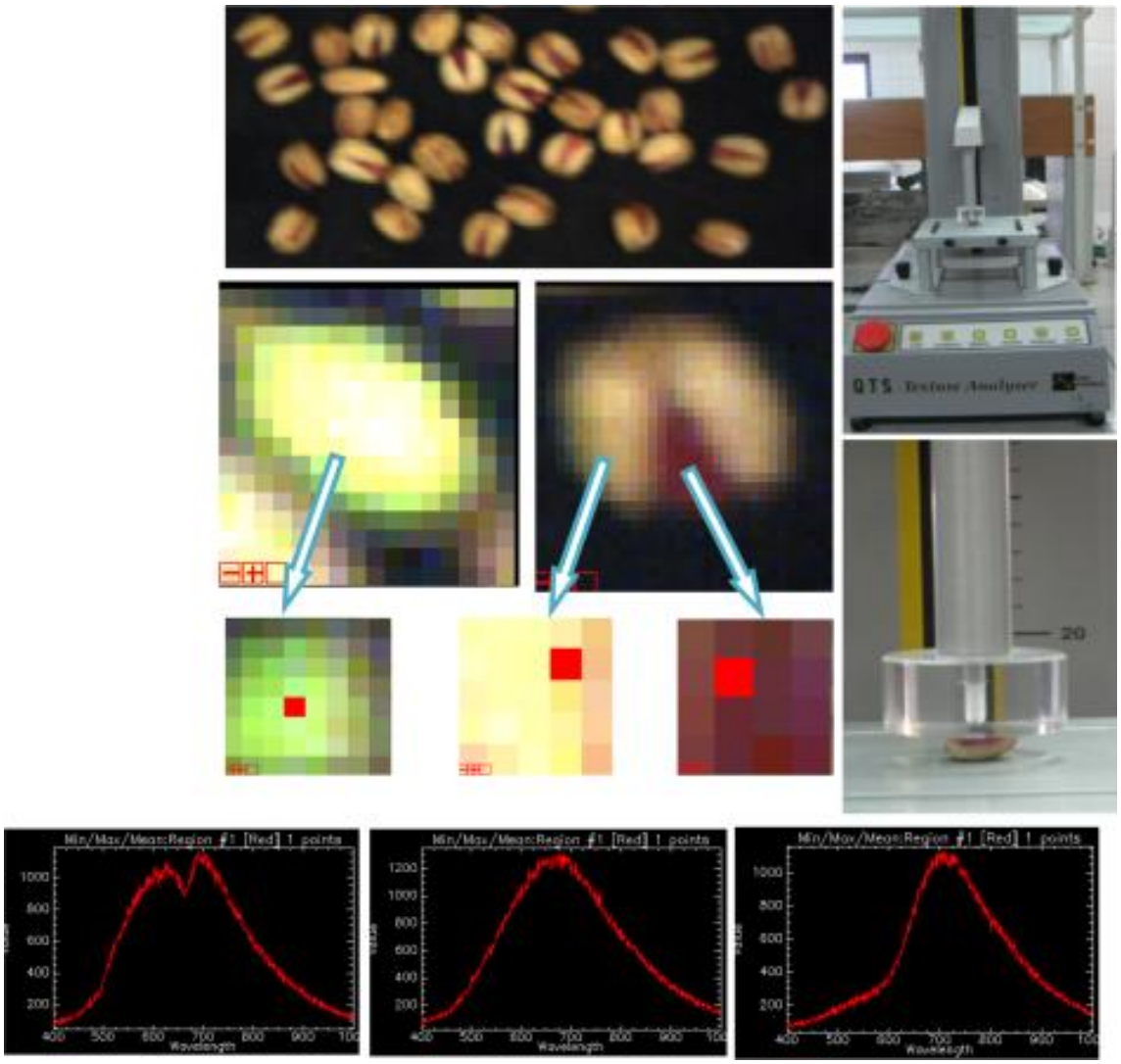

Fig. 1 Texture analyzer instrument and typical hyperspectral image and spectrum of roasted pistachio kernels in the range 400–1000 nm

lens, spectrograph (spectroscopic resolution of 5 nm), CCD camera (Basler A312f, effective resolution of 580 × 580 pixels by 12 bits), acquisition system, moving table, and illumination via fibre optics. Each scan was taking approximately 10–15 s. Figure 1 shows a typical hyperspectral image and spectrum of roasted pistachio kernels. Hyperspectral images were obtained in at least five replications.

Pre-processing

The overall mean reflectance spectra of kernels were converted to absorbance values (log1/R). This approach ignores the fact that light penetration in biological tissue is more complicated than structural materials and also involves scattering [25]. In addition, the spectral pre-processing techniques are required to remove any irrelevant information including noises, uncertainties, variabilities, interactions and unrecognized features. A lot of pre-processing techniques for spectral data have been recently developed [26]. In this study, several pre-processing methods including normalization [multiplicative scatter correction (MSC), standard normal variate transformation (SNV)], smoothing (median filter, Savitzky–Golay and Wavelet filter level 2) and differentiation (first derivative and second derivative) were used. Normalization is designed to remove multiplicative spectral effects. In normalization, the spectral vector is transformed into unit length [27]. Several smoothing techniques have been proposed to remove random noise from spectra, including moving average filters and the Savitzky–Golay algorithm [28, 29]. It is crucial to select the proper smoothing window width. Smoothing is also necessary in order to optimize the signal-to-noise ratio [26, 30]. In general, it is combined with

other pre-processing methods to accomplish the de-noising [26, 31, 32]. Wavelet transforms (WT) is a very popular kind of operation today due to its widespread application in chemometrics and signal processing. In this method, the raw signals are decomposed into a series of different frequency signal blocks. The small Wavelet coefficients presenting noise and background signals are removed [33]. Another pre-processing method known as the first and second derivative is used to remove background and increase spectral resolution [26]. First derivatives are applied to remove additive baseline effects while second derivatives are used to remove sloped additive baselines [27].

Data analysis

In this study, samples' spectra were isolated from hyperspectral images by ENVI software (version 4.7, Research System Inc. (RSI), USA). All pre-processing techniques were carried out using ParLeS software (version 3.1, the University of Sydney, Australia) [34]. To make models at PLSR and ANN methods, ParLeS software and Matlab R2009a (version 7.8.0.347, MathWorks Inc., USA) were used, respectively. Principal component analysis (PCA) was performed for a maximum of two principal components. PCA showed that there was one spectral outlier in calibration data set. This sample was identified and removed before modeling by PLSR and ANN. PLSR based on ten segments were used as the main method for developing of calibration sets. To apply PLSR, prior to develop determination models, sample data was randomly divided to calibration set (70% of the whole samples) and validation set (30% of the whole samples). In PLSR method, pre-processing techniques were done on calibration and validation set separately. Validation set was used to evaluate the robustness of the developed models. The coefficient of determination (R^2), the root mean square error of prediction (RMSEP) and the ratio of the standard deviation of the response variable to RMSEP [known as relative performance determinant (RPD)] were calculated. Generally, a powerful model should have low RMSEP and high R^2 between the predicted and measured values of each property. Moreover, low number of PLSR factors and high RPD are desirable. An RPD between 1.5 and 2 means that the model can discriminate low from high values of the response variable; a value between 2 and 2.5 indicates that course quantitative predictions are possible, and a value between 2.5 and 3 or above corresponds to good and excellent prediction accuracy, respectively [29, 35, 36].

To apply artificial neural network (ANN), a two-layer feed-forward network with sigmoid hidden neurons and linear output neurons was used. The network was trained with Levenberg–Marquardt back propagation algorithm, unless there is not enough memory, in which case scaled conjugate gradient back propagation (trainscg) was used. During training, momentum and gradient values were $0.001–1\times10^{10}$, and $1–1\times10^{-10}$, respectively. The training process was carried on for 1000 epochs. Totally 824 data were experimentally collected and randomly divided into three partitions for training (70% of data), validating (15% of data) and testing (15% of data) of the developed network. In ANN method, pre-processing techniques were done for all data. Due to the high volume of hyperspectral data, 1 neuron in hidden layer was used for prediction of the moisture content and textural characteristics of pistachio kernels. Data from hyperspectral imaging and moisture content from experimental method were considered as input and output of neural network respectively. Then R^2 and RMSEP were used to compare the performance of different ANN architectures.

Results and discussions

Tables 1 and 2 show the moisture content and textural characteristics of roasted pistachio kernels and the summary statistics for all samples selected in each data set, respectively. In this study, the range of moisture content, fracture force, hardness, apparent modulus of elasticity and compressive energy were 0.5–2.26%, 35.61–81.98 N, 43.52–82.76 N, 21.68–47 N/mm and 117.10–280.73 N.mm, respectively.

Interpretation of hyperspectral data

Figure 2a–c show the typical reflectance spectra of different parts of roasted pistachio nut at wavelength range of 400–1000 nm, respectively. It can be seen that the spectra of shell (Fig. 2a), whole kernel (Fig. 2b) and internal part of kernel (Fig. 2c) show different patterns. As illustrated, the obtained spectra have some reflectance peaks at specific wavelengths. Figure 2c shows the internal part of kernel has 2 peaks at 630 and 690 nm, while shell and whole kernel have 1 peak at 670 and 720 nm, respectively and the peak of whole kernel is sharper than shell (Fig. 2a, b). It can be seen the intensity of reflectance is different for shell, whole kernel and internal part of kernel. The highest and the lowest intensity were for internal part of kernel and whole kernel, respectively. The spectral slope of internal part is higher than shell and whole kernel at 500–700 nm (Fig. 2a–c). Kim et al. [37] found one peak for apple at 430–930 nm at reflectance and fluorescence hyperspectral imaging. Weinstoc et al. [17] identified 3 peaks at 1000, 1200 and 1450 nm for corn at reflectance hyperspectral imaging.

Effect of roasting conditions on the spectra of pistachio kernels

Figure 3a–c show the effect of temperature, air velocity and time of roasting on the spectra of pistachio kernels. It

Table 1 Moisture content and textural properties of pistachio kernels at different temperatures, times and air velocities of roasting

Temperature (°C)	Time (min)	Air velocity (m/s)	Moisture content (%)	Fracture force (N)	Hardness (N)	Apparent modulus of elasticity (N/mm)	Compressive energy (N.mm)
90	20	0.5	2.12 ± 0.10	44.90 ± 9.26	76.95 ± 6.49	37.65 ± 2.19	230.55 ± 4.51
90	20	1.5	2.18 ± 0.11	71.29 ± 10.21	71.70 ± 8.38	47 ± 2.99	171.60 ± 13.70
90	20	2.5	2.26 ± 0.10	73.03 ± 5.26	73.59 ± 5.40	38.07 ± 4.33	240.32 ± 20.18
90	35	0.5	1.75 ± 0.08	75.48 ± 1.49	77.50 ± 5.83	39.94 ± 6.65	232.56 ± 21.30
90	35	1.5	1.98 ± 0.07	81.98 ± 5.92	82.76 ± 6.19	43.27 ± 6.44	280.73 ± 28.70
90	35	2.5	1.50 ± 0.07	77.77 ± 7.69	79.21 ± 7.53	38.50 ± 1.24	242.70 ± 25.88
90	50	0.5	1.50 ± 0.08	78.15 ± 5.89	80.42 ± 3.67	41.59 ± 3.60	243.09 ± 24.52
90	50	1.5	2.02 ± 0.12	64.96 ± 9.17	80.42 ± 2.41	41.39 ± 0.03	247.28 ± 11.44
90	50	2.5	1.50 ± 0.09	80.00 ± 10.25	80.76 ± 10.20	30.78 ± 6.15	231.65 ± 2.71
120	20	0.5	2.04 ± 0.10	76.90 ± 5.19	81.28 ± 0.93	40.10 ± 7.44	253.98 ± 5.46
120	20	1.5	1.46 ± 0.08	59.05 ± 9.29	63.93 ± 4.28	41.37 ± 6.94	199.06 ± 14.29
120	20	2.5	2.19 ± 0.04	46.45 ± 5.05	73.27 ± 1.40	36.63 ± 8.61	194.75 ± 13.74
120	35	0.5	1.50 ± 0.06	60.38 ± 7.28	61.91 ± 4.80	31.6 ± 1.66	188.80 ± 1.04
120	35	1.5	1.59 ± 0.07	65.86 ± 10.21	68.06 ± 7.68	24.98 ± 3.87	189.31 ± 10.08
120	35	2.5	0.50 ± 0.02	56.13 ± 1.01	63.13 ± 6.59	21.76 ± 4.45	166.90 ± 5.71
120	50	0.5	1.00 ± 0.02	41.35 ± 8.28	59.86 ± 2.71	28.92 ± 2.83	154.68 ± 6.52
120	50	1.5	1.44 ± 0.01	59.55 ± 2.95	69.86 ± 4.72	33.15 ± 3.09	200.52 ± 5.98
120	50	2.5	0.75 ± 0.01	56.68 ± 9.32	56.97 ± 9.25	21.68 ± 6.49	151.51 ± 8.79
150	20	0.5	1.75 ± 0.10	46.59 ± 4.38	48.04 ± 7.18	28.89 ± 0.94	127.52 ± 14.04
150	20	1.5	1.24 ± 0.11	35.61 ± 2.52	43.52 ± 5.99	22.19 ± 1.23	119.98 ± 2.19
150	20	2.5	1.26 ± 0.08	43.14 ± 7.80	47.17 ± 1.03	24.25 ± 8.08	117.10 ± 6.51
150	35	0.5	1.50 ± 0.10	40.05 ± 6.54	44.97 ± 6.78	23.72 ± 6.87	125.13 ± 9.82
150	35	1.5	1.08 ± 0.10	58.72 ± 4.38	59.69 ± 2.74	23.61 ± 6.84	158.36 ± 8.60
150	35	2.5	1.00 ± 0.09	39.33 ± 6.25	45.26 ± 6.99	22.28 ± 8.65	144.21 ± 13.58
150	50	0.5	0.75 ± 0.05	39.57 ± 2.21	43.62 ± 0.92	23.54 ± 6.66	134.92 ± 12.72
150	50	1.5	0.82 ± 0.06	50.32 ± 8.82	55.10 ± 8.87	27.15 ± 3.35	148.80 ± 9.50
150	50	2.5	0.50 ± 0.04	25.54 ± 5.94	37.59 ± 5.70	21.22 ± 1.75	101.18 ± 13.18

Table 2 Statistical results on both calibration and validation sets for prediction of moisture content and textural properties of roasted pistachio kernels at PLSR method

Characteristic	Calibration set					Validation set				
	Mean	SD	Median	Minimum	Maximum	Mean	SD	Median	Minimum	Maximum
Moisture content (w.b. %)	1.61	0.49	1.50	0.50	2.26	1.26	0.45	1.26	0.75	1.98
Fracture force (N)	58.16	14.15	58.72	35.61	77.77	59.39	17.16	59.09	39.33	81.98
Hardness (N)	65.84	12.5	68.06	43.52	81.28	63.31	15.94	63.93	43.62	82.76
Apparent modulus of elasticity (N/mm)	31.88	8.44	31.6	21.68	47.00	32.45	7.96	30.78	22.28	43.27
Compressive energy (N.mm)	187.38	46.82	188.8	117.10	253.98	190.06	54.44	199.06	127.52	280.73

SD standard deviation

can be seen that roasting increased the reflectance of pistachio kernels at the range of 400–640 and 670–1000 nm, whereas the reflectance of pistachio kernels decreased at 640–670 nm, though these changes were intangible. As shown in Fig. 3a, increasing the roasting temperature led to increase the reflectance of pistachio kernels. During the roasting, moisture content decreases and amount of reflectance increases. Figures 3b and 2c show the effect of roasting air velocity and time on the spectra of pistachio kernels. It can be observed these parameters cause to change the reflectance of pistachio kernels at the

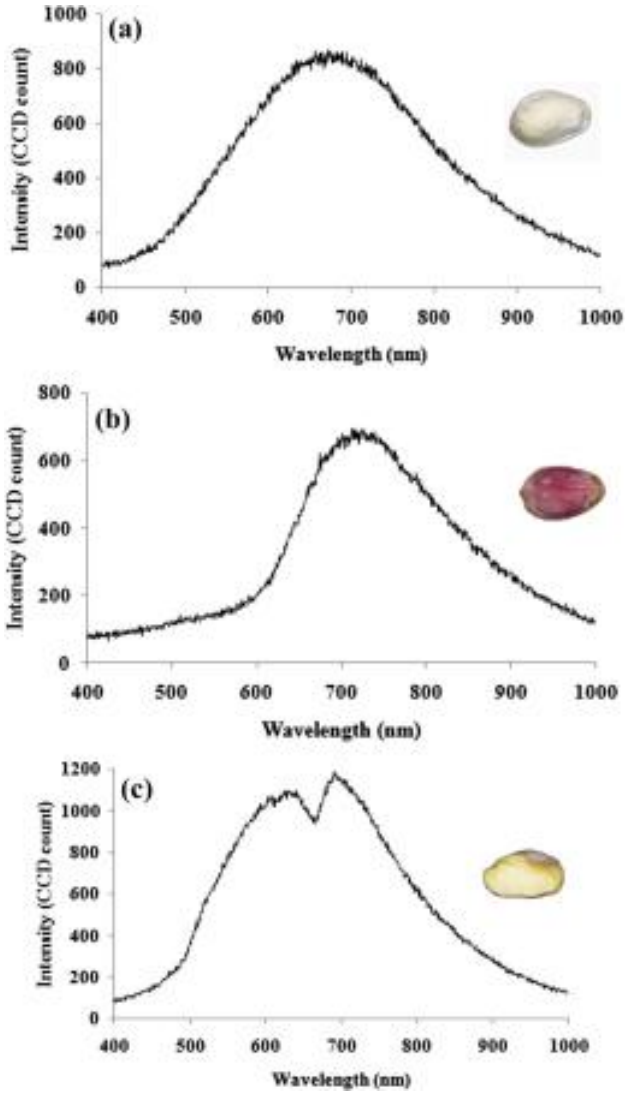

Fig. 2 Original reflectance spectra of **a** pistachio shell, **b** whole pistachio kernel and **c** internal part of pistachio kernel

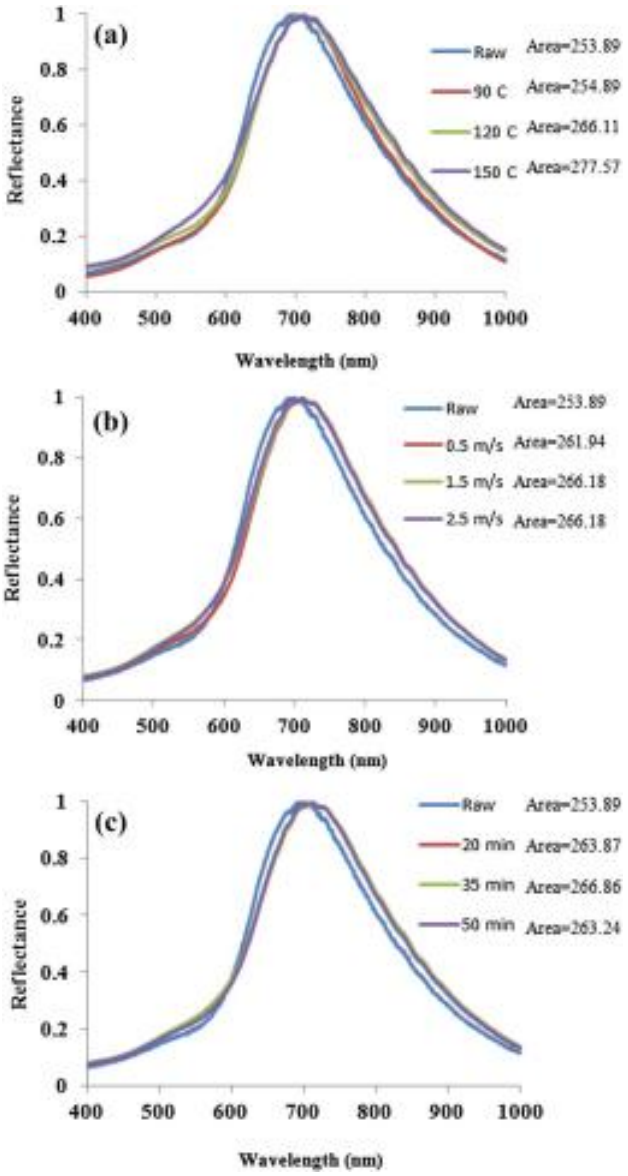

Fig. 3 Effect of roasting temperature (**a**), air velocity (**b**) and time (**c**) on the spectra of pistachio kernels

mentioned ranges, although these changes don't show sensible difference at various roasting time and air velocity.

Effects of different pre-processing techniques

The results of PLSR and ANN models with several combinations of preprocessing techniques for moisture content and textural characteristics of roasted pistachio kernels are summarized in Tables 3 and 4. In the absence of pre-processing techniques, low correlation coefficients were observed for prediction of all studied parameters. However, with the use of pre-processing techniques, in some models, correlation coefficient and RPD increased and the RMSEP decreased. Although PLSR models could predict moisture content and textural properties of pistachio kernels, but it could not make good predictions for these properties, because of low R^2 and RPD values and high RMSEP value (Tables 3, 4). Cogdill et al. [16] used transmission hyperspectral imaging (750–1090 nm), PLSR and PCR methods for prediction of moisture content of corn. They reported PLSR has higher potential in predicting moisture content of corn comparing to PCR.

Moisture content

Table 3 shows the results obtained for PLSR and ANN models on prediction of moisture content of roasted pistachio kernels. It can be seen that ANN models can predict moisture content of roasted pistachio kernels better than PLSR

Table 3 The prediction results of moisture content with different pre-processing techniques

Pre-processing method	PLSR				ANN	
	No. of factor	RPD	RMSEP	R^2	RMSEP	R^2
Original data	4	0.57	0.787	0.242	0.238	0.816
SNV, median filter, D^1	5	0.94	0.478	0.473	0.238	0.804
MSC, median filter, D^1	5	0.98	0.459	0.478	0.219	0.824
SNV, median filter, D^2	5	0.46	0.982	0.528	0.376	0.530
MSC, median filter, D^2	4	0.45	1.005	0.525	0.292	0.690
SNV, Wavelet, D^1	4	0.85	0.524	0.517	**0.179**	**0.907**
MSC, Wavelet, D^1	1	1	0.448	0.251	0.244	0.820
SNV, Wavelet, D^2	9	0.78	0.572	0.051	0.284	0.742
MSC, Wavelet, D^2	5	0.39	1.153	0.055	0.314	0.689
SNV, Savitzky–Golay, D^1	2	0.84	0.535	0.432	0.269	0.767
MSC, Savitzky–Golay, D^1	2	0.89	0.505	0.333	0.308	0.676
SNV, Savitzky–Golay, D^2	1	0.74	0.605	0.226	0.199	0.873
MSC, Savitzky–Golay, D^2	1	1.04	0.432	0.233	0.130	0.767

R^2 coefficient of determination, *RMSEP* the root mean square error of prediction, *RPD* the ratio of the standard deviation of the response variable to the RMSEP, *SNV* standard normal variate transformation, *MSC* multiplicative scatter correction, D^1 first derivative, D^2 second derivative

models. In total, PLSR models showed low RPD and R^2. For all samples, RPD was lower than 1.5, indicating that developed models do not give an accurate prediction for moisture content. The best results with ANN method were achieved using a combination of SNV, Wavelet and D^1 for predicting moisture content with $R^2 = 0.907$ and RMSEP = 0.179 (Table 3). Cogdill et al. [16] developed a technique for creating calibrations to predict the constituent concentrations of single maize kernels from NIR hyperspectral transmission data in the range of 750–1090 nm. PLSR and PCR were used to develop predictive calibration models for moisture and oil contents. Standard normal variate, detrending, multiplicative scatter correction, wavelength selection by genetic algorithm, and no preprocessing were compared for their effect on predictive model performance. The predictive calibration model for moisture content achieved a best standard error of cross-validation (SECV) of 1.20%, with RPD of 2.74. The best results for prediction of oil content achieved an SECV of 1.38%, with an RPD of only 1.45. Huang et al. [38] used the hyperspectral imaging technology and PLSR for prediction the moisture content of maize kernels during the drying. They predicted the moisture content with the uniformity (indirect) and uniformity directly. Better prediction results were achieved using the direct method (RP = 0.848 and RMSEP = 2.73) than the indirect method (RP = 0.521 and RMSEP = 10.96).

Fracture force

ANN models could predict the fracture force as well and better than the moisture content and other textural characteristics. In terms of pre-processing methods, MSC was better against SNV to predict the fracture force for smoothing techniques. Nevertheless, better results were achieved using a combination of MSC, Savitzky–Golay and D^1 for predicting the fracture force with $R^2 = 0.957$ and RMSEP = 3.386 (Table 4). The ANN model preprocessed with the combination of SNV, Savitzky–Golay and D^1 had the same R^2, but RMSE value was higher than the best model (RMSE = 3.405) (Table 4). PLSR models could predict the fracture force but they didn't give an accurate prediction because of high RMSEP and low RPD. The best PLSR model was obtained with $R^2 = 0.823$, RMSEP = 12.37, RPD = 1.38 and 3 PLSR factors.

Hardness

The results indicated that ANN models can predict the hardness better than PLSR models. The best results with PLSR models were achieved using a combination of SNV, Wavelet and D^1 with $R^2 = 0.643$, RMSEP = 10.78, RDP = 1.48 and 2 PLSR factors (Table 4). However, due to high RMSEP and low R^2 and RPD, it can be mentioned that prediction of hardness values with ANN model was not sufficiently desirable; however it was better than PLSR models. The best results with ANN models were achieved using a combination of SNV, Wavelet and D^2 with $R^2 = 0.876$ and RMSEP = 5.216 (Table 4). Williams et al. [19] used the NIR hyperspectral imaging (960–1662 nm and 1000–2498 nm) for distinguishing between hard, intermediate and soft maize samples. They found that PCA can illustrate a distinct difference between glassy and floury endosperm along principal component. Subsequently, they applied partial least squares discriminant

Table 4 The prediction results of textural characteristics and moisture content of pistachio kernels with different pre-processing techniques

Textural characteristics	Fracture force (N)						Hardness (N)						Compressive energy (N.MM)						Apparent modulus of elasticity (N/s)					
Pre-processing methods	PLSR				ANN		PLSR				ANN		PLSR				ANN		PLSR				ANN	
	No. of factor	RPD	RMSEP	R^2	RMSEP	R^2	No. of factor	RPD	RMSEP	R^2	RMSEP	R^2	No. of factor	RPD	RMSEP	R^2	RMSEP	R^2	No. of factor	RPD	RMSEP	R^2	RMSEP	R^2
Original data	1	1.16	14.76	0.44	7.48	0.88	4	1.49	10.70	0.51	6.57	0.82	4	1.41	38.49	0.64	23.12	0.79	4	1.03	7.72	0.44	3.58	0.86
SNV, median filter, D^1	7	1.28	13.37	0.56	14.33	0.45	2	1.33	12.10	0.45	6.74	0.77	1	1.16	46.86	0.55	23.36	0.78	7	1.42	5.61	0.49	3.49	0.82
MSC, median filter, D^1	7	1.25	13.65	0.56	7.11	0.82	2	1.33	12.02	0.46	8.23	0.66	1	1.14	47.85	0.55	35.99	0.67	5	1.39	5.71	0.50	5.47	0.70
SNV, median filter, D^2	6	0.34	50.22	0.31	7.50	0.80	7	0.31	52.09	0.35	8.56	0.63	7	0.34	160.02	0.32	31.85	0.68	6	0.30	26.64	0.59	4.56	0.78
MSC, median filter, D^2	7	0.33	50.99	0.31	7.38	0.78	7	0.30	52.94	0.36	5.26	0.86	6	0.34	162.37	0.33	21.52	0.82	6	0.29	27.07	0.61	3.94	0.77
SNV, Wavelet, D^1	3	1.38	12.37	0.82	7.67	0.79	2	1.48	10.78	0.64	7.25	0.74	2	1.33	41.05	0.54	27.32	0.73	2	1.27	6.29	0.30	**2.37**	**0.92**
MSC, Wavelet, D^1	6	1.15	14.89	0.29	8.83	0.70	1	1.15	13.89	0.34	12.77	0.64	1	1.09	49.76	0.45	**15.76**	**0.91**	1	1.05	7.56	0.29	3.44	0.85
SNV, Wavelet, D^2	5	0.54	31.39	0.01	9.89	0.61	2	0.47	33.88	0.00	**5.22**	**0.88**	5	0.52	102.08	0.01	34.73	0.57	5	0.45	17.80	0.07	4.76	0.70
MSC, Wavelet, D^2	2	0.32	54.03	0.52	6.29	0.85	4	0.27	58.56	0.54	9.94	0.52	5	0.33	178.66	0.32	35.20	0.55	2	0.27	18.96	0.11	3.04	0.86
SNV, Savitzky–Golay, D^1	8	1.32	12.95	0.76	3.40	0.96	1	0.94	16.97	0.43	6.19	0.82	1	0.97	55.91	0.54	17.96	0.87	1	0.98	8.14	0.32	4.29	0.75
MSC, Savitzky–Golay, D^1	9	1.49	11.47	0.64	**3.39**	**0.96**	2	1.40	11.39	0.45	8.89	0.64	1	1.25	43.69	0.53	24.34	0.77	1	1.17	6.79	0.33	4.83	0.82
SNV, Savitzky–Golay, D^2	1	0.95	17.99	0.49	7.57	0.78	1	0.90	17.71	0.45	6.56	0.79	1	0.94	57.90	0.56	29.98	0.74	1	0.95	8.42	0.34	4.16	0.79
MSC, Savitzky–Golay, D^2	4	1.25	13.62	0.43	6.51	0.84	1	1.13	14.05	0.36	7.70	0.73	1	1.22	44.62	0.48	24.40	0.76	1	0.99	8.04	0.31	3.43	0.84

R^2 coefficient of determination, *RMSEP* the root mean square error of prediction, *RPD* the ratio of the standard deviation of the response variable to the RMSEP, *SNV* standard normal variate transformation, *MSC* multiplicative scatter correction, D^1 first derivative, D^2 second derivative)

analysis (PLS-DA) for model classification. The hardness values were predicted with RMSEP of 0.18 in 960–1662 nm and RMSEP of 0.29 in 1000–2498 nm wavelength range.

Apparent modulus of elasticity

Table 4 shows the results of PLSR and ANN methods for prediction of the apparent modulus of elasticity. It can be observed again ANN models predicted the apparent modulus of elasticity better than PLSR models. In the case of ANN, the best model was found to be the one with preprocessing techniques containing combination of SNV, Wavelet and D^1 with $R^2 = 0.921$ and RMSEP = 2.366 (Table 4).

Compressive energy

The results of PLSR and ANN methods for prediction of compressive energy are shown in Table 4. The best results with PLSR models were achieved without preprocessing ($R^2 = 0.643$, RMSEP = 38.490 and RPD = 1.41). High RMSEP and low RPD indicated inability of PLSR models in predicting compressive energy (Table 4). In the case of ANN, the best model was found using the combination of MSC, Wavelet and D^1 as preprocessing techniques with $R^2 = 0.907$ and RMSEP = 15.757 (Table 4).

Conclusions

The feasibility of utilizing Vis/NIR hyperspectral imaging (400–1000 nm) combined with different preprocessing methods to nondestructive prediction of moisture content and textural characteristics of roasted pistachio kernels was investigated. Employing pre-processing methods, in some cases, increased correlation coefficient and RPD of the developed model while it decreased the RMSEP, suggesting that preprocessing techniques would enhance the models'performance. Based on the obtained data, SNV method would generate slightly better results than MSC. In all cases, the results revealed that ANN models would predict moisture content and textural characteristics of roasted pistachio kernels better than PLSR models. ANN models could predict fracture force as well and better than the moisture content and other textural characteristics. The best obtained models for moisture content ($R^2 = 0.907$, RMSEP = 0.179) and apparent modulus of elasticity ($R^2 = 0.921$, RMSEP = 2.366) with the combination of SNV, Wavelet and D^1 and for fracture force ($R^2 = 0.957$, RMSEP = 3.386,) with MSc, Savitzky–Golay and D^1, for hardness ($R^2 = 0.876$, RMSEP = 5.216) with SNV, Wavelet and D^2 and for compressive energy ($R^2 = 0.907$, RMSEP = 15.757) with MSc, Wavelet and D^1 showed high prediction ability of Vis/NIR hyperspectral imaging. The findings of this study demonstrate the predictive ability of Vis/NIR hyperspectral imaging combined with selected chemometric tools. This technology can be successfully used as a non-destructive tool for measuring moisture content and textural characteristics of pistachio kernels at different roasting conditions.

Acknowledgements The authors would like to thank Dr. Raphael A. Viscarra Rossel for providing ParLes software.

References

1. M. Bayram, Comparison of unsplit in shell and shelled kernel of the pistachio nuts. J. Food Eng. **107**(3–4), 374–378 (2011)
2. FAOSTAT. FAOSTAT database results. http://faostat.fao.org/site/339/default.aspx. Accessed 29 Sept 2017
3. M. Maskan, S. Karatas, Fatty acid oxidation of pistachio nuts stored under various atmospheric conditions & different temperatures. J. Sci. Food Agric. **77**, 334–340 (1998)
4. S. Saklar, Optimization of hazelnut roasting process by using response surface methodology. PhD thesis, METU, Ankara (1999)
5. M. Özdemir, F.G. Seyhan, A.K. Bakan, G. Ilter, O. Devres, Analysis of internal browning of roasted hazelnuts. Food Chem. **73**, 191–196 (1999)
6. A.D. Demir, K. Cronin, The thermal kinetics of texture change and the analysis of texture variability for raw and roasted hazelnuts. IJFST **39**, 371–383 (2004)
7. J.G. Woodroof, *Tree Nuts: Production Processing Products*, 2nd edn. (AVI, Westport, 1979)
8. R.Y.Y. Chiou, T.T. Tsai, Characteristics of peanut proteins during roasting as affected of initial moisture. J. Agric. Food Chem. **37**, 1377–1381 (1989)
9. L.B. Emily, D.B. Terri, A.W. Lester, Effect of cultivar and roasting method on composition of roasted soybeans. J. Sci. Food Agric. **89**(5), 821–826 (2009)
10. J.F.V. Vincent, Application of fracture mechanics to the texture of food. Eng. Fail Anal. **11**, 695–704 (2004)
11. J.A. Abbott, Quality measurement of fruits and vegetables. Postharvest Biol. Technol. **5**, 207–225 (1999)
12. T. Mohammadi-Moghaddam, S.M.A. Razavi, M. Taghizadeh, A. Sazgarnia, Sensory and instrumental assessment of roasted pistachio nut/kernel by partial least square (PLS) regression analysis: effect of roasting conditions. J. Food Sci. Technol. **53**(1), 370–380 (2016)
13. A.A. Gowen, C.P. O'Donnell, P.J. Cullen, G. Downey, J.M. Frias, Hyperspectral imaging—an emerging process analytical tool for food quality and safety control. Trends Food Sci. Technol. **18**(12), 590–598 (2007)
14. D. Sun (ed.), *Hyperspectral Imaging for Food Quality Analysis and Control* (Academic Press, Elsevier, San Diego, 2010)
15. D. Lorente, N. Aleixos, J. Gmez-Sanchis, S. Cubero, O.L. Garcia-Navarrete, J. Blasco, Recent advances and applications of hyperspectral imaging for fruit and vegetable quality assessment. Food Bioprocess Technol. **5**(4), 1121–1142 (2012)
16. R.P. Cogdill, Jr..C.R. Hurburgh, G.R. Rippke, Single-kernel maize analysis by near-infrared hyperspectral imaging. TASABE **47**(1), 311–320 (2004)
17. B.A. Weinstock, J. Janni, L. Hagen, S. Wright, Prediction of oil and oleic acid concentrations in individual corn (*Zea mays* L.)

kernels using near infrared reflectance hyperspectral imaging and multivariate analysis. Appl. Spectrosc. **60**(1), 9–16 (2006)
18. B. Zhu, L. Jiang, F. Jin, L. Qin, A. Vogel, Y. Tao, Walnut shell and meat differentiation using fluorescence hyperspectral imagery with ICA-kNN optimal wavelength optimal wavelength selection. Sens. Instrum. Food Qual. Saf. **1**, 123–131 (2007)
19. P. Williams, P. Geladi, G. Fox, M. Manley, Maize kernel hardness classification by near infrared (NIR) hyperspectral imaging and multivariate data analysis. Anal. Chim. Acta **653**, 121–130 (2009)
20. S.R. Delwiche, I.C. Yang, M.S. Kim, Hyperspectral imaging for detection of black tip damage in wheat kernels, in *Proceedings of SPIE–The International Society for Optical Engineering*, vol 7315, (2009)
21. J. Xing, S. Symons, M. Shahin, D. Hatcher, Detection of sprout damage in Canada Western Red Spring wheat with multiple wavebands using visible/near-infrared hyperspectral imaging. Biosyst. Eng. **106**, 188–194 (2010)
22. X. Zhang, F. Liu, Y. He, X. Li, Sensor application of hyperspectral imaging and chemometric calibrations for variety discrimination of maize seeds. Sensors **12**, 17234–17246 (2012)
23. F. Goktas Seyhan, Effect of soaking on salting and moisture uptake of pistachio nuts (*Pistachia vera* L.) from Turkiye. GIDA **28**(4), 395–400 (2003)
24. S.M.A. Razavi, M.R. Edalatian, Effect of moisture content and compression axis on physical and mechanical properties of pistachio kernel. Int. J. Food Prop. **15**, 507–517 (2012)
25. A.M. Davies, A. Grant, Review: near-infra-red analysis of food. IJFST **22**, 191–207 (1987)
26. H. Cen, Y. He, Theory and application of near infrared reflectance spectroscopy in determination of food quality. Trends Food Sci. Technol. **18**, 72–83 (2007)
27. H. Swierenga, A.P. De Weijer, R.J. Van Wijk, L.M.C. Buydens, Strategy for constructing robust multivariate calibration models. Chemom. Intell. Lab. Syst. **49**, 1–17 (1999)
28. T. Næs, T. Isaksson, T. Fearn, T. Davies, *A User-Friendly Guide to Multivariate Calibration and Classification* (NIR Publications, Charlton, 2004)
29. B.M. Nicolaï, K. Beullens, E. Bobelyn, A. Peirs, W. Saeys, K.I. Theron, J. Lammertyn, Nondestructive measurement of fruit and vegetable quality by means of NIR spectroscopy: a review. Postharvest Biol. Technol. **46**, 99–118 (2007)
30. J.H. Perkin, B. Tenge, D.E. Honigs, Resolution enhancement using an approximate-inverse Savitzky-Golay smooth. Spectrochim. Acta B **43**, 575–603 (1998)
31. M.J.C. Pontes, S.R.B. Santos, M.C.U. Araujo, L.F. Almeida, R.A.C. Lima, E.N. Gaiao, U.T.C.P. Souto, Classification of distilled alcoholic beverages and verification of adulteration by near infrared spectrometry. Food Res. Int. **39**, 182–189 (2006)
32. L. Wang, F.S.C. Lee, X.R. Wang, Y. He, Feasibility study of quantifying and discriminating soybean oil adulteration in camellia oils by attenuated total reflectance MIR and fiber optic diffuse reflectance NIR. Food Chem. **95**, 529–536 (2006)
33. J. Yoon, B. Lee, C. Han, Calibration transfer of near-infrared spectra based on compression of wavelet coefficients. Chemom. Intell. Lab. Syst. **64**, 1–14 (2002)
34. R.A.V Rossel, ParLeS: software for chemometric analysis of spectroscopic data. Chemom. Intell. Lab. Syst., **90**, 72–83 (2008)
35. P.C. William, D.G. Sobering, How do we do it: a brief summary of the method we use in developing near infrared calibrations, in Near Infrared Spectroscopy: The Future Waves, ed. by A.M.C. Davies, P. Williams (NIR Publications, Chichester, 1996), pp. 185–188
36. W. Saeys, A.M. Mouazen, H. Ramon, Potential for onsite and online analysis of pig manure using visible and near infrared reflectance spectroscopy. Biosyst. Eng. **91**, 393–402 (2005)
37. M.S. Kim, Y.R. Chen, P.M. Mehl, Hyperspectral reflectance and fluorescence imaging system for food quality and safety. ASABE **44**(3), 721–729 (2001)
38. M. Huang, W. Zhao, Q. Wang, M. Zhang, Q. Zhu, Prediction of moisture content uniformity using hyperspectral imaging technology during the drying of maize kernel. Int. Agrophys. **29**(1), 39–46 (2015)